The ISME Journal (2016) 10, 693–706

www.nature.com/ismej

ORIGINAL ARTICLE

Global distribution and vertical patterns of a prymnesiophyte–cyanobacteria obligate symbiosis

Ana M Cabello[1], Francisco M Cornejo-Castillo[1], Nicolas Raho[2], Dolors Blasco[1], Montserrat Vidal[3], Stéphane Audic[4,5], Colomban de Vargas[4,5], Mikel Latasa[6], Silvia G Acinas[1] and Ramon Massana[1]

[1]*Department of Marine Biology and Oceanography, Institut de Ciències del Mar (CSIC), Barcelona, Spain;* [2]*Department of molecular Biology, Universidad Autónoma de Madrid, Madrid, Spain;* [3]*Departament of Ecology, University of Barcelona, Barcelona, Spain;* [4]*Station Biologique de Roscoff, Université Pierre et Marie Curie - Paris 6, Roscoff, France;* [5]*Laboratoire Adaptation et Diversité en Milieu Marin, CNRS, UMR 7144, Roscoff, France and* [6]*Centro Oceanográfico de Gijón (IEO), Gijón, Spain*

A marine symbiosis has been recently discovered between prymnesiophyte species and the unicellular diazotrophic cyanobacterium UCYN-A. At least two different UCYN-A phylotypes exist, the clade UCYN-A1 in symbiosis with an uncultured small prymnesiophyte and the clade UCYN-A2 in symbiosis with the larger *Braarudosphaera bigelowii*. We targeted the prymnesiophyte–UCYN-A1 symbiosis by double CARD-FISH (catalyzed reporter deposition-fluorescence *in situ* hybridization) and analyzed its abundance in surface samples from the MALASPINA circumnavigation expedition. Our use of a specific probe for the prymnesiophyte partner allowed us to verify that this algal species virtually always carried the UCYN-A symbiont, indicating that the association was also obligate for the host. The prymnesiophyte–UCYN-A1 symbiosis was detected in all ocean basins, displaying a patchy distribution with abundances (up to 500 cells ml^{-1}) that could vary orders of magnitude. Additional vertical profiles taken at the NE Atlantic showed that this symbiosis occupied the upper water column and disappeared towards the Deep Chlorophyll Maximum, where the biomass of the prymnesiophyte assemblage peaked. Moreover, sequences of both prymnesiophyte partners were searched within a large 18S rDNA metabarcoding data set from the *Tara*-Oceans expedition around the world. This sequence-based analysis supported the patchy distribution of the UCYN-A1 host observed by CARD-FISH and highlighted an unexpected homogeneous distribution (at low relative abundance) of *B. bigelowii* in the open ocean. Our results demonstrate that partners are always in symbiosis in nature and show contrasted ecological patterns of the two related lineages.
The ISME Journal (2016) **10,** 693–706; doi:10.1038/ismej.2015.147; published online 25 September 2015

Introduction

Symbiosis between cyanobacteria and eukaryotic organisms is a widespread phenomenon reported both in land and in aquatic systems (Rai *et al.*, 2002). In the marine environment, cyanobacteria appear associated with multicellular organisms, such as ascidians and sponges, and with single-celled organisms, such as diatoms, dinoflagellates, radiolarians and tintinnids (Carpenter and Foster, 2002; Foster *et al.*, 2006). These findings derive from microscopic observations and often the mutual benefit between the host and the symbiont is poorly understood. Generally, it is assumed that the cyanobacteria provides organic carbon to the host through photosynthesis, while the host provides a stable and secure environment. Diazotrophic cyanobacteria symbionts can, in addition, provide nitrogen-derived metabolites through N_2 fixation, as has been demonstrated in some diatom species (Foster *et al.*, 2011).

A related and particular symbiosis has been recently described between two uncultured picoplankters, a small (⩽3 μm) prymnesiophyte and the unicellular diazotrophic cyanobacteria UCYN-A (Thompson *et al.*, 2012). Genomics revealed that UCYN-A lacked key metabolic pathways commonly shared by diazotrophic cyanobacteria, such as oxygenic photosynthesis and the Calvin cycle, suggesting it was an obligate symbiont (Zehr *et al.*, 2008; Tripp *et al.*, 2010). Indeed, nano secondary ion mass spectrometry demonstrated that the symbiont gave fixed nitrogen to the host and obtained organic carbon in return (Thompson *et al.*, 2012). The 18S rDNA prymnesiophyte sequence, identified by single cell analysis (Thompson *et al.*, 2012), was identical to an environmental sequence from the South Pacific (Shi *et al.*, 2009) and related (98.2%) to *Braarudosphaera bigelowii*, a coastal nanoplanktonic

Correspondence: AM Cabello or R Massana, Department of Marine Biology and Oceanography, Institut de Ciències del Mar (CSIC), Passeig Marítim de la Barceloneta 37-49, Barcelona 08003, Spain. E-mail: amcabello@icm.csic.es or ramonm@icm.csic.es
Received 6 March 2015; revised 15 July 2015; accepted 21 July 2015; published online 25 September 2015

coccolithophore (Hagino *et al*., 2009). Later, endosymbiotic UCYN-A was also discovered in *B. bigelowii* by transmission electron microscopic observations (Hagino *et al*., 2013). Phylogenetic analyses using the UCYN-A nitrogenase (*nifH*) gene revealed at least three distinct clades, UCYN-A1, -A2 and -A3 (Thompson *et al*., 2014), and highlighted specificity between host and symbiont pairings, suggesting co-evolution between symbionts and hosts (Bombar *et al*., 2014; Thompson *et al*., 2014). Thus the clade UCYN-A1 was associated with an open ocean small prymnesiophyte (hereafter UCYN-A1 host), and the clade UCYN-A2 was associated with the coastal and larger *B. bigelowii* (hereafter UCYN-A2 host), while no host has been yet proposed for UCYN-A3.

Environmental surveys of *nifH* genes indicated a rather global distribution of this symbiosis in the oceans (Moisander *et al*., 2010). Further reports showed that the distinct UCYN-A clades were widespread and often coexisted (Thompson *et al*., 2014). Nevertheless, microscopic observations of the symbiosis or sequencing data of the prymnesiophytes verifying this widespread distribution are still scarce. Recently, a double CARD-FISH (catalyzed reporter deposition-fluorescence *in situ* hybridization) approach targeting UCYN-A and prymnesiophyte cells allowed visualization and quantification of this association in the North Atlantic (Krupke *et al*., 2014a, b). Later, the same double CARD-FISH technique but specifically targeting the two different prymnesiophyte host phylotypes made it possible to distinguish both types of associations and to observe their co-occurrence in the subtropical South Atlantic (Cornejo-Castillo *et al*., submitted). The emerging picture derived from the above studies was that the prymnesiophyte–UCYN-A association showed a tendency for being more abundant in oligotrophic warm waters, but the environmental drivers explaining its distribution are still poorly understood. In this sense, quantifying the symbiosis by both CARD-FISH and 18S rDNA metabarcoding in a large set of samples covering a wide geographic range help evaluating accurately its distribution in marine ecosystems.

In this work, we studied the distribution of UCYN-A1 and UCYN-A2 hosts in samples representative of the World's major oceans. First, we targeted the prymnesiophyte–UCYN-A1 symbiosis by double CARD-FISH using the specific probe for the UCYN-A1 host (Cornejo-Castillo *et al*., submitted) and the general probe UCYN-A732, targeting all clades of UCYN-A (Krupke *et al*., 2013). This FISH setup was used to quantify cell abundances in surface waters tracked during the MALASPINA expedition, to analyze vertical distributions in the NE Atlantic near the Iberian Peninsula and to evaluate whether the host can appear without the cyanobacteria. Second, we analyzed the global distribution of both hosts within an 18S rDNA metabarcoding data set from the *Tara*-Oceans expedition sampled at surface and deep chlorophyll maximum (DCM) depths (De Vargas *et al*., 2015). The aim of this work was to confirm the broad distribution of the prymnesiophyte–UCYN-A association, evaluate its putative ecological niche and provide further evidence about the obligatory dependence of both symbiont and host.

Materials and methods

Oceanographic cruises

We analyzed data from three independent cruises. The MALASPINA circumnavigation expedition took place from December 2010 to July 2011 on board the R/V *Hespérides* and tracked subtropical and tropical latitudes of the Atlantic, Indian and Pacific oceans (see Supplementary Figure S1a for a map of stations). The *Tara*-Oceans expedition (Karsenti *et al*., 2011) took place from September 2009 to March 2012 on board the *Tara* schooner and encompassed a different track on the same oceans plus the Mediterranean Sea and subantarctic waters (Supplementary Figure S1b). The INDEMARES 0710 cruise took place in summer 2010 (28 July–15 August) on board the R/V *Thalassa* (IFREMER/IEO) in the NE Atlantic near the Iberian peninsula (Supplementary Figure S1a). For MALASPINA and INDEMARES, sampling and acquisition of hydrological variables are detailed below. Seawater sampling, DNA extract collection and 18S rDNA sequencing for the *Tara*-Oceans expedition is described in detail elsewhere (De Vargas *et al*., 2015).

Sampling procedures during MALASPINA and INDEMARES cruises

During the MALASPINA cruise, surface samples (~3 m) for CARD-FISH and chlorophyll *a* analysis were collected with a 30-l Niskin bottle (Sea-Bird Electronics, Bellevue, WA, USA) at around noon in 59 stations (minimum bottom depth ~2000 m). Conductivity–temperature–depth casts were performed from surface to mesopelagic depths with a Seabird 911Plus probe mounted on a 24-bottle Niskin rosette and water was taken at several depths for nutrient analysis. In the INDEMARES cruise, vertical profiles were taken at offshore stations in the Avilés canyon (stations A–B) and the Galician Bank (stations C–D). Casts were performed after sunset with a conductivity–temperature–depth profiler fitted with a Fluorometer (ECO-AFL, WET-Labs, Philomath, OR, USA) and a 24-bottle Niskin rosette. Based on the downcast fluorescence profile, seawater was collected at 7–8-m depths from below the DCM to surface (~5 m), with higher frequency above the DCM. For chlorophyll *a* determination, aliquots of 250 ml (MALASPINA) or 2-l (INDEMARES) were filtered through Whatman GF/F filters (25 mm diameter, Sigma-Aldrich, Buchs, Switzerland) and stored at −20 °C until extraction on board or in the lab, respectively. Samples for inorganic nutrients were drawn into polyethylene vials and kept frozen until analysis. For the CARD-FISH assay, 95 ml

aliquots for MALASPINA or 45 ml aliquots for INDEMARES were fixed with 37% formaldehyde (2 or 4% final concentration, respectively), filtered on 0.6 μm pore-size polycarbonate filter (25 mm diameter; DHI, Hørsholm, Denmark) and kept frozen until processed.

Chlorophyll a and inorganic nutrient measurements

During MALASPINA, pigments were extracted by placing the filters in 5–7 ml of 90% acetone at 4 °C for 24 h and determining the fluorescence of the extract in a Turner Designs fluorometer (Turner Designs Inc., Sunnyvale, CA, USA; Yentsch and Menzel, 1963). A chlorophyll *a* standard (Sigma-Aldrich) was used to calibrate the fluorometer and no phaeophytin correction was applied. For INDEMARES samples, pigments were extracted with 90% acetone, sonicated, kept at −20 °C for 24 h and cleared by filtration through GF/F filters. Total chlorophyll *a* was determined by high-performance liquid chromatography following the procedure described by Latasa (2014).

In MALASPINA samples, nitrate (NO_3^-) concentration was measured spectrophotometrically with a Skalar autoanalyzer (Skalar SANplus, Skalar Analytical B. V., Breda, The Netherlands) following the standard procedures (Grasshoff *et al*., 1999; Moreno-Ostos, 2012), and phosphate (PO_4^{3-}) concentration was measured manually with a Perkin Elmer spectrophotometer (Perkin Elmer, Waltham, MA, USA). For INDEMARES, both nutrients were measured with a Skalar autoanalyzer. Detection limits were 0.02 μM for NO_3^- and 0.01 μM for PO_4^{3-}. N/P ratios were calculated from the ratio between significant slope values ($P<0.05$) of nitrate and phosphate across the nutricline. Dissolved organic nitrogen and phosphorus were estimated as the difference between total nitrogen and phosphorus and inorganic values. Total nitrogen and phosphorus concentrations were determined by nitrate and phosphate measures carried out after alkaline and acidic persulphate oxidation, respectively (Grasshoff *et al*., 1999; Moreno-Ostos, 2012).

Double CARD-FISH assay

The double CARD-FISH assay was already used for the same symbiosis (Krupke *et al*., 2014a) and followed the Multi-color CARD-FISH protocol (Pernthaler *et al*., 2004). Filters were embedded in 0.1% low gelling point agarose to minimize cell loss and treated with lysozyme (37 °C, 1 h) and acromopeptidase (37 °C, 0.5 h) to permeabilize cell covers. For the first CARD-FISH step, we used probe UPRYM69 (5′-CACATAGGAACATCCTCC-3′) specific for the UCYN-A1 host. Design, specificity and optimization to ensure maximal stringency of the probe are detailed in Cornejo-Castillo *et al*. (submitted). This probe was combined with oligonucleotide helpers (sequences contiguous to the probe region (Helper A-PRYM 5′-GAAAGGTGCTGA AGGAGT-3′; Helper B-PRYM 5′-AATCCCTAGTCGG CATGG-3′)) and a competitor (having one mismatch in the probe region (5′-CACATTGGAACATCCTCC-3′)). Filter pieces (1/8 of the filter) were covered with hybridization buffer (40% deionized formamide, 0.9 M NaCl, 20 mM Tris-HCl pH 8, 0.01% sodium dodecyl sulfate (SDS), and 20 mg ml^{-1} blocking reagent (Roche Diagnostic Boehringer, Basel, Switzerland)) containing a mixture of the horseradish peroxidase-labeled probe, helpers and competitor each at 5 ng μl^{-1}. After incubating at 46 °C overnight, two washing steps of 10 min were carried out at 48 °C in a buffer (56 mM NaCl, 5 mM EDTA, 0.01% SDS, 20 mM Tris-HCl pH 8), and filters were equilibrated in phosphate-buffered saline (PBS) buffer for 15 min at room temperature. Tyramide signal amplification (TSA) was done for 40 min at room temperature in the dark in a solution of 1 × PBS, 2 M NaCl, 1 mg ml^{-1} blocking reagent, 100 mg ml^{-1} dextran sulfate, 0.0015% H_2O_2 and 4 μg ml^{-1} Alexa 488-labeled tyramide. Filters were transferred to PBS for 20 min, rinsed with distilled water and air-dried. Before the second hybridization, probe peroxidases were inactivated with 0.01 M HCl for 10 min at room temperature in the dark (Pernthaler *et al*., 2004) and filters were rinsed twice with MilliQ water and air-dried. The second CARD-FISH used the probe UCYN-A732, targeting both UCYN-A1 and -A2 cells, and the hybridization conditions described in Krupke *et al*. (2013). Filters were embedded in the hybridization buffer (50% formamide, 0.9 M NaCl, 20 mM Tris-HCl pH 8, 0.01% SDS, 10 mg ml^{-1} Blocking reagent and 100 mg ml^{-1} dextrane sulfate) with the probe and helpers at 0.16 ng μl^{-1}, incubated at 35 °C for 3 h, then rinsed in a washing buffer (as described above but with 9 mM NaCl) at 37 °C, and TSA was at 46 °C in the same solution described above but using 1 μg ml^{-1} Alexa 594-tyramide. Filters were counterstained with 5 μg ml^{-1} DAPI (4′, 6- diamidino-2-phenylindole), mounted in antifading reagent (77% glycerol, 15% VECTASHIELD and 8% 20 × PBS) and kept frozen.

In a few samples, double CARD-FISH was carried out targeting *B. bigelowii*, using the specific UBRADO69 probe (5′-CACATTGGAACATCCTCC-3′) together with the same helpers as before and a different competitor (5′-CACATAGGAACATCCTCC-3′) (Cornejo-Castillo *et al*., submitted), and probe UCYN-A732 under the same hybridization and amplification conditions described above. In INDEMARES samples, the class-specific probe PRYM02 (Simon *et al*., 2000) was applied to target all prymnesiophytes in addition to the specific probe UPRYM69. Hybridization and TSA conditions for probe PRYM02 were as described for probe UPRYM69 with modified hybridization temperature (35 °C) and NaCl concentration in the washing buffer (37 mM).

Epifluorescence microscopy counts

Filters were observed by epifluorescence microscopy (Olympus BX61, Olympus America Inc., Center Valley, PA, USA) at ×1000 under ultraviolet (DAPI

signal of the nucleous), blue light (green labeled host cells with Alexa 488) or green light (red labeled symbionts with Alexa 594) excitations. Counts of hybridized cells were performed in 3–4 transects (~8.0×0.1 mm^2 each) across the filter piece, which were analyzed twice. A first inspection was carried out under blue light to count host cells and examine the presence of associated symbionts by switching to green light. A second analysis was carried out under green light to detect free symbionts. Detection limit was about 2 cells ml^{-1} (calculated assuming only one counted cell). Cell counts included four categories: (1) labeled host cells in association with labeled UCYN-A cells, (2) non-labeled host cells with labeled UCYN-A cells, (3) labeled hosts without symbionts (non-associated hosts), and (4) labeled non-associated UCYN-A cells (free symbionts). Prymnesiophyte cells were classified into five size classes (1–2, 2–3, 3–4, 4–5 and >5 μm) by measurements with an ocular micrometer (Olympus America Inc.). Micrographs were taken with an Olympus DP72 camera (Olympus America Inc.) attached to the microscope.

Similarity search of prymnesiophyte sequences in the Tara-Oceans expedition

The *Tara*-Oceans expedition studied protist diversity in several size fractions by 18S rDNA metabarcoding (De Vargas *et al*., 2015). Here we analyzed the V9 18S rDNA Illumina reads derived from the 0.8–5 μm size fraction taken at surface and DCM in 40 stations. High-quality reads were clustered at 100%, derived operational taxonomic units (OTUs) were taxonomically classified to remove OTUs from Archaea, Bacteria and Metazoa. From the final OTU table (73 samples with 87 millions reads), we noted the total number of reads and the number of prymnesiophyte reads per sample. Then, we did BLAST searches to identify the two prymnesiophyte phylotypes using sequences Biosope T60.034 (FJ537341) and *B. bigelowii* Genotype III (AB250784) as seeds. Two OTUs identical to the seeds were identified, represented by 62 423 and 29 803 reads for the UCYN-A1 and UCYN-A2 hosts, respectively. These two phylotypes were also found in the 5–20 μm size fraction but at lower abundance (1010 and 3244 reads, respectively), so we decided to use here only the data for the 0.8–5 μm size fraction. V9 rDNA data set is available at Pangaea under http://doi.pangaea.de/10.1594/PANGAEA.843018. Identifiers of the OTUs were 07f330a1423-bc41xc2473a1a93a47f94b for the UCYN-A1 host and c2716f4902d581e7907e3c0a33917c17 for the UCYN-A2 host.

Results

Microscopic observations

We targeted the prymnesiophyte–UCYN-A1 symbiosis by double CARD-FISH in 59 surface samples from all major ocean basins taken during the MALASPINA expedition and in 30 water column samples from vertical profiles in the NE Atlantic taken in the INDEMARES cruise (see Supplementary Figure S1a for a map of stations). Symbiosis was detected in about 50% of these samples. The labeling with probe UPRYM69 allowed us to distinguish the specific host from the other prymnesiophyte cells (Figure 1a). Most cells targeted by probe UPRYM69 (86%, $n = 2030$ cells) were associated with UCYN-A. These prymnesiophyte cells were always very small and had a coherent size among samples. About 60% of the cells observed were between 1 and 2 μm in size, 38% within 2–3 μm and 2% within 3–4 μm, resulting in a typical size of ~2.5 μm.

The specific prymnesiophyte was associated with one UCYN-A cell in most cases, but some carried two symbionts (Figure 1b). This was rarely seen in MALASPINA samples, only in 5 out of the 24 samples and always at very low abundance (up to 2% of the observed cells). On the other hand, host cells with two symbionts were more frequent in INDEMARES samples, being detected in virtually all samples along the four vertical profiles analyzed. On average, 25% of the observed host cells in station A carried two UCYN-A cells, with lower values in the other casts (2.4% in station B, 6.4% in station C and 5.0% in station D).

We never observed UCYN-A cells associated with non-prymnesiophyte eukaryotes. In a few cases, we detected UCYN-A cells hosted by larger prymnesiophyte-like cells not labeled by probe UPRYM69 (Supplementary Figure S2). In some of these samples, the larger host was later positively targeted with the UBRADO69 probe, verifying that it was *B. bigelowii* (Figure 1c). All *B. bigelowii* cells counted ($n = 17$) were within the 4–5 μm size fraction.

To characterize the dependence of the prymnesiophyte host to UCYN-A1, we categorized the samples based on the observations of free partners (Supplementary Table S1). In general, free partners were more frequent in samples that had high symbiosis abundances (131 ± 141 cells ml^{-1}, $n = 22$) than in samples with low symbiosis abundances (32 ± 27 cells ml^{-1}, $n = 14$). Samples where free partners were not detected presented the lowest symbiosis abundances (15 ± 14 cells ml^{-1}, $n = 11$). Moreover, by combining the counts from the 47 samples with symbiosis, we observed that non-associated host abundances were positively related to free symbiont abundances (Figure 2a). The similar abundances of both free partners strongly suggests that they derive from the same association, being likely detached owing to sample processing (Supplementary Figure S3). There was no significant relationship between partners likely detached and symbiotic states (Figure 2b), implying that the extent of the putative disruption depended on how particular samples were handled. A rough estimate suggests that between 10 and 20% of the original symbiosis could be disrupted by sample manipulation.

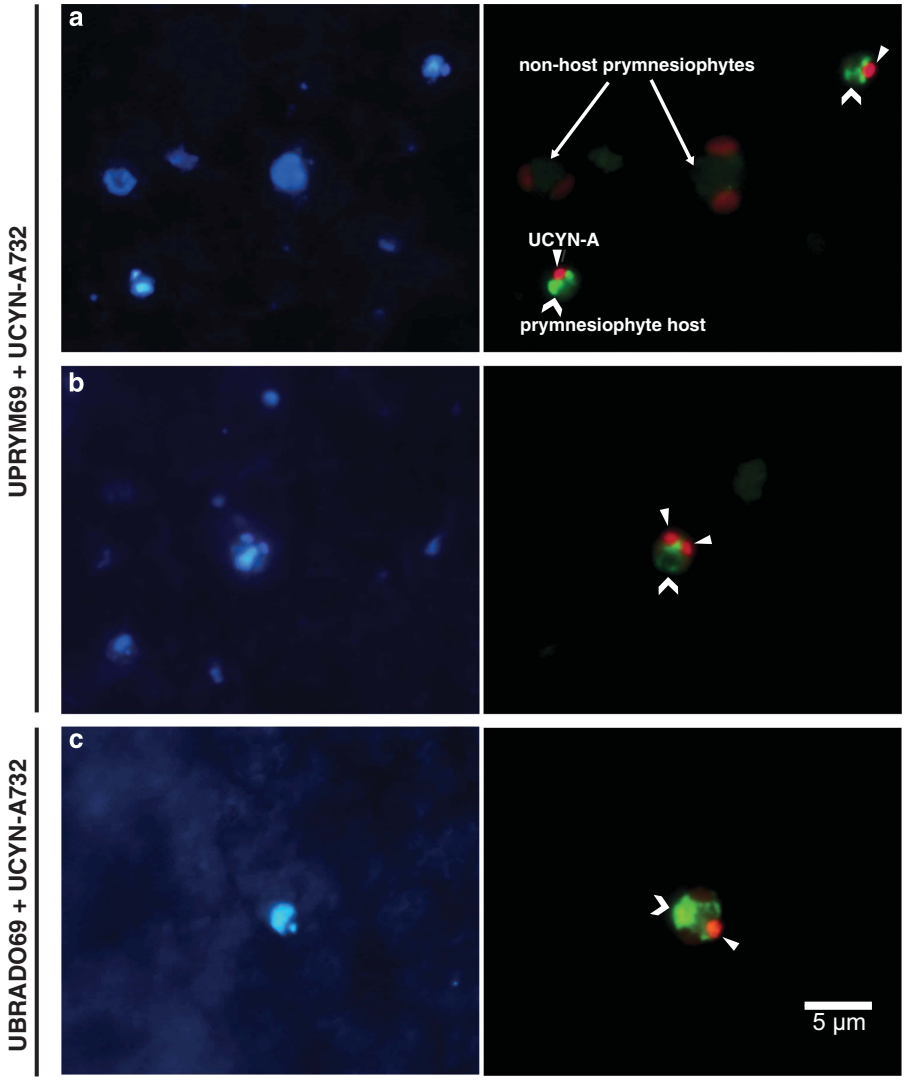

Figure 1 Epifluorescence microscopy images of the double CARD-FISH assay. Left panels correspond to DAPI signal (blue-labeled nucleous). Right panels correspond to the combined signal of the prymnesiophyte-specific probes (green-labeled host under blue light excitation) and the cyanobacteria (red-labeled symbiont under green light excitation). (**a**) Two prymnesiophyte host cells carrying the symbiont close to two non-host prymnesiophyte cells from MALASPINA station 64. (**b**) A prymnesiophyte host harboring two UCYN-A cells from surface of station A (INDEMARES cruise) where this type of association was frequently observed. (**c**) A *B. bigelowii* cell targeted by the UBRADO69 probe from MALASPINA station 68.

Global distribution in surface waters

The abundance of the prymnesiophyte–UCYN-A1 association in surface waters was analyzed by double CARD-FISH in 59 MALASPINA and 3 INDEMARES samples. CARD-FISH counts showed that the symbiosis was present in all major ocean basins usually in patches of neighboring stations (Figure 3a). It was detected in 27 out of the 62 surface samples collected in geographic sites with different environmental settings (Supplementary Figure S4). There were some hotspots of high abundance in the NE Atlantic (476 cells ml^{-1} in station A), near the Hawaiian archipelago (128 and 213 cells ml^{-1} in stations 100 and 101, respectively) and in the Indian Ocean close to South Africa (140 cells ml^{-1} in station 45) or Australia (338 and 397 cells ml^{-1} in stations 69 and 64, respectively). Excluding these six stations, the averaged cell counts for the symbiosis was 28 cells ml^{-1} (s.d. = 25; $n = 21$).

We occasionally observed UCYN-A cells associated with larger prymnesiophytes non-targeted by the UPRYM69 probe (Supplementary Figure S2). In two of the five samples where this was seen, we did an additional hybridization with probe UBRADO69, specific for UCYN-A2 hosts. These larger prymnesiophytes were labeled with this new double CARD-FISH setup, showing that they were the UCYN-A2 hosts. Counts of these larger prymnesiophytes were 8 cells ml^{-1} in the eastern subtropical North Atlantic (station 144), and 18 cells ml^{-1} in the southeast Indian Ocean close to Australia (station 68), and in both stations they co-occurred with UCYN-A1 hosts.

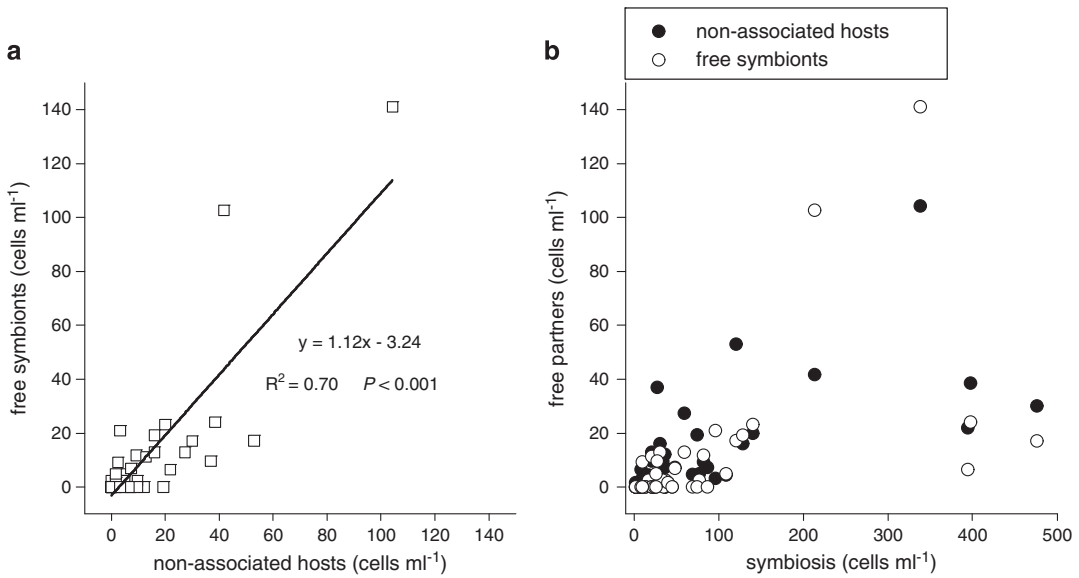

Figure 2 Relationship between cell count categories in samples where the prymnesiophye–UCYN-A1 symbiosis was detected. (**a**) Abundances of non-associated hosts versus free symbionts. (**b**) Abundances of symbiosis versus free partner cells.

The two UCYN-A hosts were then searched in the 18S rDNA metabarcoding data set obtained from surface samples of the *Tara*-Oceans expedition. Prymnesiophytes were present in all *Tara* samples ($n = 40$) (Figure 4a) in averaged percentages of 3.9% (±3.0) of total community reads, and maximal values of ~12% in the Southern Ocean (station 85) and minimal of ~0.8% in the eastern South Pacific gyre (station 100). UCYN-A1 and UCYN-A2 hosts appeared to follow different distributions, as inferred by the contribution of their reads to total prymnesiophyte reads (Figure 3b). The UCYN-A1 host appeared in a few spots with a high relative abundance (~30% of prymnesiophytes in two South Atlantic stations), while it was barely detected (<0.1%) in 10 stations and undetected in 25 additional ones. On the other hand, the UCYN-A2 host appeared in virtually all samples (in 38 out of the 40 stations; only undetected in stations 84 and 85 from the Southern Ocean), displaying an averaged percentage of 1.2% (±0.9).

Ancillary parameters measured during the cruises did not explain clearly the presence and abundance of the prymnesiophyte–UCYN-A1 symbiosis (Supplementary Figure S4). The symbiosis was detected in a wide range of temperatures (19–29 °C), in ultraoligotrophic to eutrophic sites (chl *a* values from 0.035 to 0.65 mg m^{-3}), in phosphate ranges from 0.01 to 0.23 μM, in nitrate ranges from <0.02 to 1.38 μM and in N/P ratios from 6 to >20. Indeed, symbiosis abundances were only weakly correlated to temperature and phosphate, whereas they were not correlated with chlorophyll *a*, nitrate, N/P ratio and dissolved organic phosphorus or nitrogen (Figure 5). In order to constrain the occurrence of the symbiosis, we took into account all surface samples and compared its abundance in samples inside and outside a given range of the environmental variables (Table 1). Abundances were significantly higher in samples with temperatures <25 °C and phosphate <0.08 μM. No differences in abundances were found between samples with nitrate concentrations below and above the median value observed in all samples (0.27 μM) or between samples with N/P ratios below or above 16. Moreover, symbiosis abundances were not significantly different in oligotrophic, mesotrophic or eutrophic waters, although they were significantly lower in ultraoligotrophic stations.

Vertical distribution pattern in the water column

The vertical distribution of the prymnesiophyte–UCYN-A1 symbiosis was studied in detail in four vertical profiles in the NE Atlantic (Figure 6). A stratified water column was observed in all cases with a DCM peak coupled to the beginning of the nutricline and depths above the DCM having low nitrate and phosphate concentrations (0.023 ± 0.025 μM NO_3^-; 0.075 ± 0.013 μM PO_4^{3-}). At selected depths, symbiosis counts together with total prymnesiophyte counts were obtained by double and single CARD-FISH assays, respectively. In all profiles, UCYN-A1 host cells occupied the upper water column and decreased towards the DCM, where they disappeared. The decrease in symbiosis abundances appeared more coupled to the beginning of the fluorescence gradient than to the beginning of the nutricline. On the contrary, the other prymnesiophyte cells, not involved in symbiosis, peaked at the DCM and were present throughout the photic water column. Station B lacked the surface samples, but its vertical pattern was consistent with the other three profiles. The abundance and contribution of the UCYN-A1 host varied between the two regions sampled.

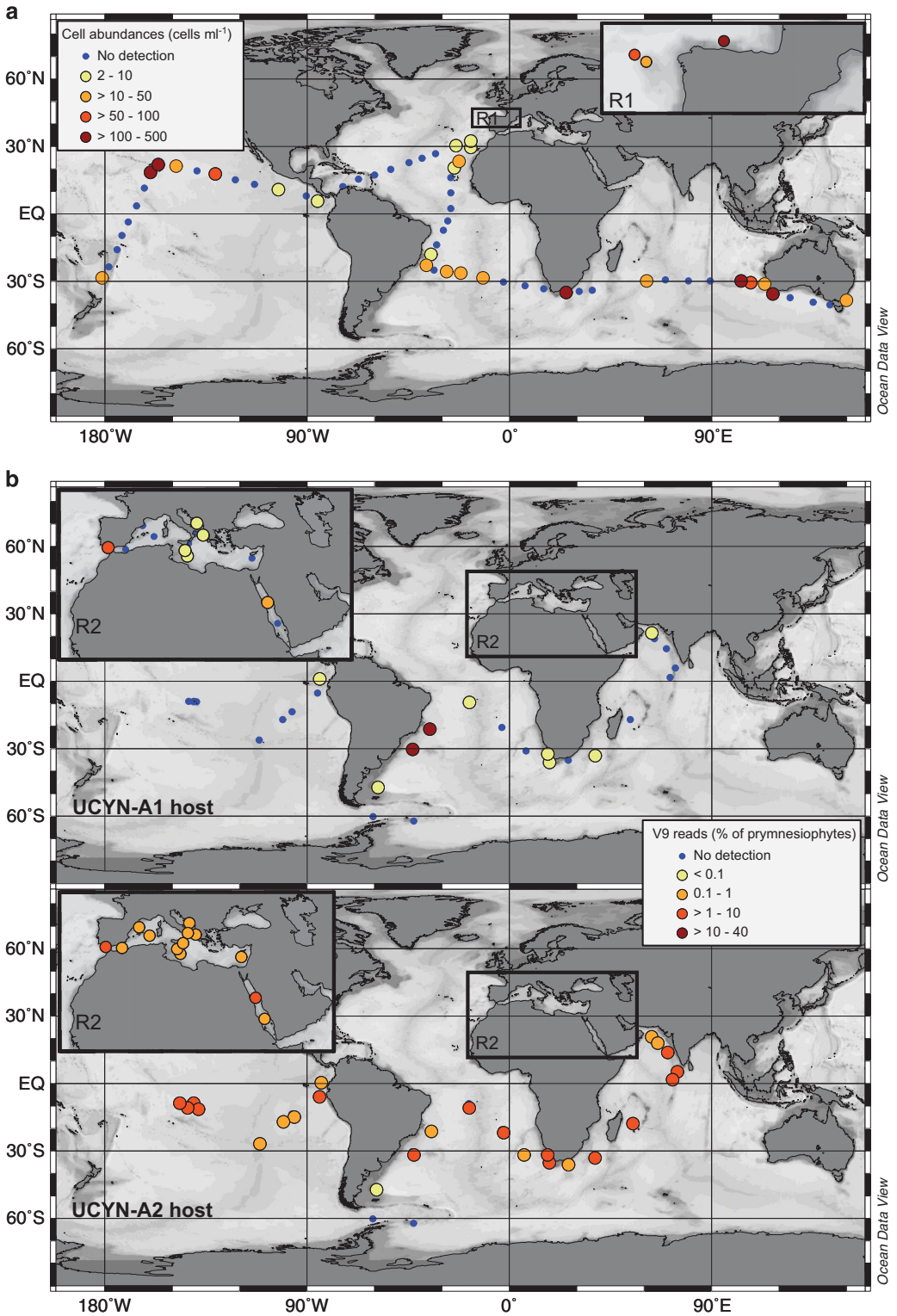

Figure 3 Global distribution of prymnesiophyte hosts in surface waters. (**a**) Cell abundances of the prymnesiophyte–UCYN-A1 symbiosis along the MALASPINA and INDEMARES cruises determined by double CARD-FISH using UPRYM69 and UCYN-A732 probes. (**b**) Relative abundances of V9 reads of UCYN-A1 host (upper panel) and UCYN-A2 host (lower panel) to total prymnesiophytes along the *Tara*-Oceans expedition.

Highest abundances were seen in the upper water column of station A (435 cells ml^{-1} on average) in the Avilés canyon region, where they represented on average 70% of the prymnesiophyte cells (up to 86% at 5 m). In the Galician Bank region, UCYN-A1 host abundances (40–80 cells ml^{-1} on average) had a lower contribution to total prymnesiophytes (8–16% on average).

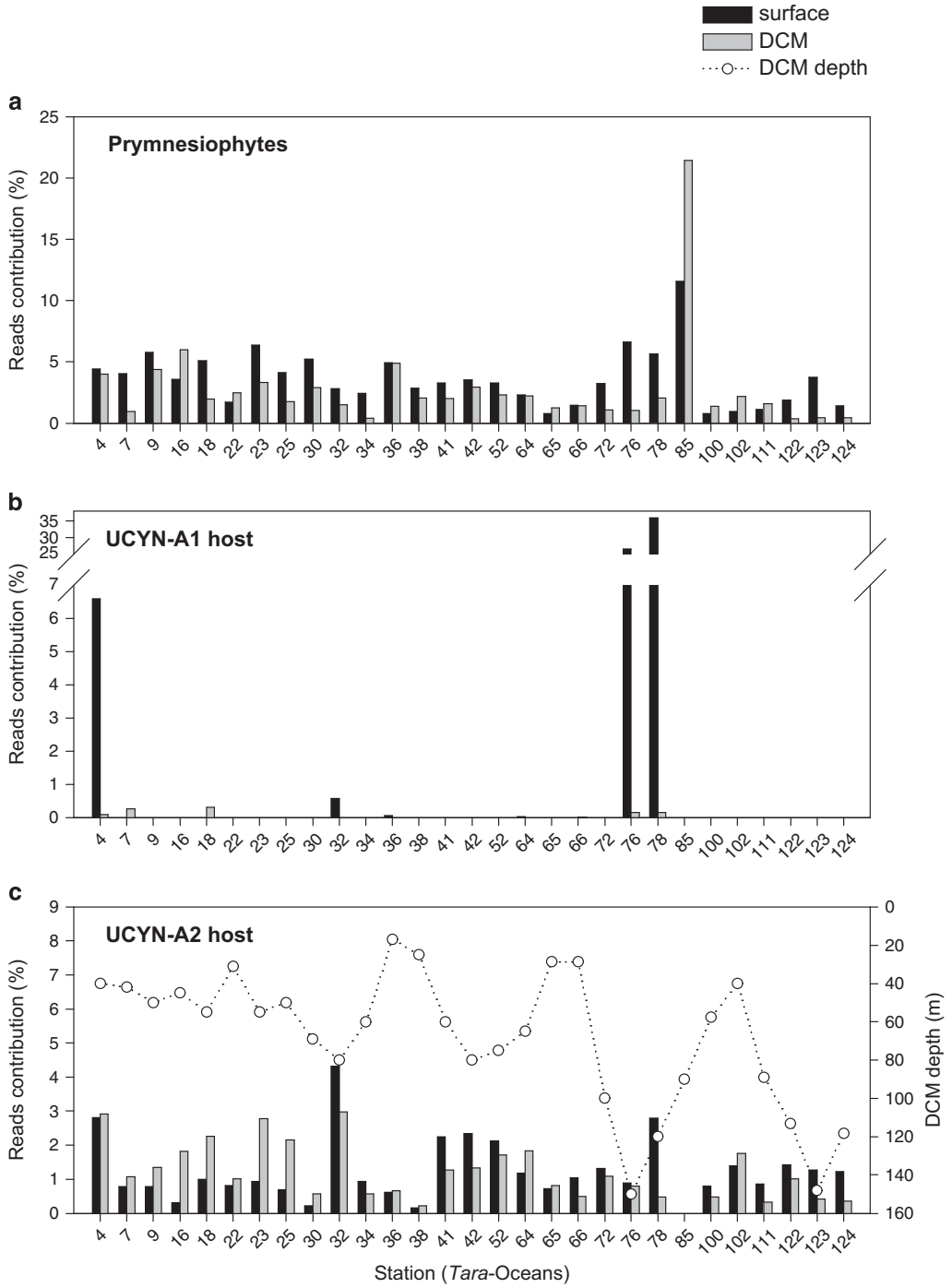

Figure 4 Contribution of prymnesiophytes to total community reads (**a**) and contribution of UCYN-A1 host (**b**) and UCYN-A2 host (**c**) to total prymnesiophyte reads at surface and DCM depths of *Tara*-Oceans stations (V9 rDNA metabarcoding data). DCM depth was plotted in panel (**c**). Only stations having both surface and DCM samples are shown (29 out of 40). In the 11 stations not shown here, the percentage of prymnesiophytes to total community reads at surface was similar (4.6% ± 4.3 on average).

The vertical distribution of the symbiosis could also be inferred by the contribution of UCYN-A host reads in surface versus DCM samples of the *Tara*-Oceans cruise. Considering only the stations with high UCYN-A1 host abundance in surface samples (stations 76 and 78 in the South Atlantic; station 4 in the Gibraltar Strait; and station 32 in the Red Sea), the contribution at the DCM was about 150 times lower (Figure 4b). In the other stations where UCYN-A1 host was scarce at surface, it was equally scarce at the DCM. By contrast, UCYN-A2 host was detected at similar abundance in surface and DCM samples in all stations where it appeared (averaged surface/DCM ratio of 1.38 ± 1.19; Figure 4c). The contribution of UCYN-A2 host was only significantly lower at the DCM (as compared with surface) in stations where

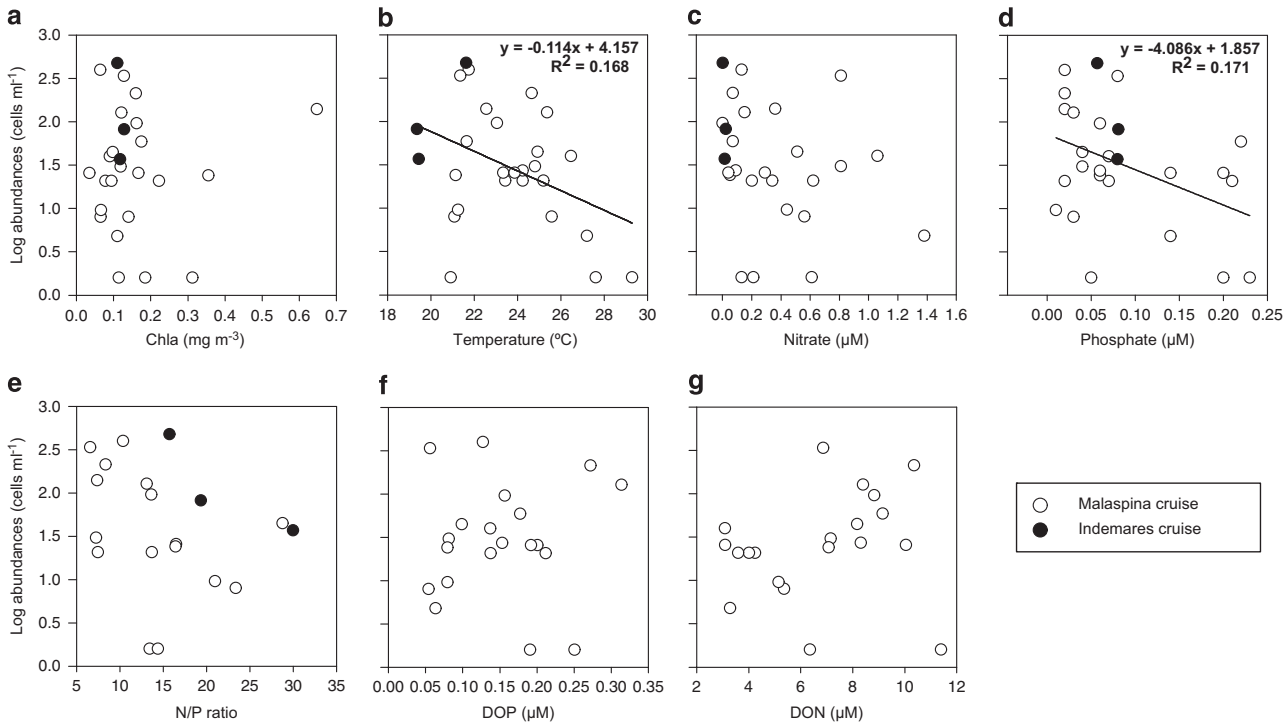

Figure 5 Cell counts of the prymnesiophyte–UCYN-A1 symbiosis versus (**a**) total chlorophyll, (**b**) temperature, (**c**) nitrate, (**d**) phosphate, (**e**) N/P ratio, (**f**) dissolved organic phosphorus (DOP) and (**g**) dissolved organic nitrogen (DON) measured in surface waters during the MALASPINA (white dots) and INDEMARES (black dots) cruises. Regression lines are plotted in cases displaying a significant relationship ($P<0.05$).

the DCM was deeper than 60 m (Mann–Whitney test; $P=0.001$, $n=29$), a difference not seen for total prymnesiophytes (Figure 4a).

Discussion

Characterization of the partnership

Microscopic observations revealed a population size spectra and phenotype consistent with previous reports, with small prymnesiophyte host cells of 2–3 µm typically with one cyanobacterial UCYN-A1 symbiont (Thompson *et al.*, 2012; Krupke *et al.*, 2014a). On the other hand, the cell size of the UCYN-A2 host in open ocean samples was 4–5 µm, clearly smaller than that described in coastal sites, about 7–10 µm (Hagino *et al.*, 2013; Thompson *et al.*, 2014). This is in agreement with a greater contribution of *B. bigelowii* reads in the 0.8–5 µm size fraction (as compared with the 5–20 µm fraction) in the *Tara*-Oceans metabarcoding data analyzed here, as well as of UCYN-A2 reads in the same smaller size fraction in metagenomic samples of the South Atlantic (Cornejo-Castillo *et al.*, submitted).

The hypothesis about the obligatory dependence of UCYN-A with its host (Tripp *et al.*, 2010; Thompson *et al.*, 2012; Bombar *et al.*, 2014) has been recently reinforced with the strong coupling observed in the transfer of carbon and nitrogen metabolites between partner cells (Krupke *et al.*, 2014b). On the other hand, the possibility of a free-living population of the host could not be evaluated as the FISH probe used in previous studies (Krupke *et al.*, 2014a) targeted the whole prymnesiophyte assemblage and not the specific host phylotypes. Our use of a specific probe for the UCYN-A1 host allowed us to validate that this association was also obligatory for the host as (i) we never observed a free-living population of targeted prymnesiophytes in the absence of UCYN-A and (ii) counts of free partner cells, when detected, were correlated, suggesting a disruption of the association owing to sample manipulation (Thompson *et al.*, 2012; Krupke *et al.*, 2013). To our knowledge, this is one of the few cases showing an obligatory dependency of a phytoplankton species and its symbiont. The high degree of specificity between partners and the reductive evolution of the UCYN-A genomes (Bombar *et al.*, 2014) are features analogous to those observed in some freshwater diatom species, which harbor N_2-fixing cyanobacteria as endosymbionts that are inseparable from the host and transferred to daughter cells during host cell division (Nakayama *et al.*, 2014). The UCYN-A symbiont of *B. bigelowii* is also an endosymbiont as observed by transmission electron microscopy (Hagino *et al.*, 2013), and it is likely that the prymnesiophyte–UCYN-A1 association presents analogous structural properties.

In our study, about 97% of the hosts carried a single UCYN-A1 cell. This supports previous observations from the North Pacific (Thompson *et al.*, 2012) and the North Atlantic (Krupke *et al.*, 2014a).

Table 1 Averaged abundances of symbiosis inside and outside of a given range of values for temperature, phosphate, nitrate, N/P ratio and chlorophyll *a*.

Variable	*Range*		*Abundances (cells ml^{-1})*				*Number of samples*	
			In range		*Out of range*		*In range*	*Out of range*
			Average	*s.d.*	*Average*	*s.d.*	n	n
Temperature	<25 °C	(*)	21	120	7	25	33	29
PO_4^{3-}	<0.08 μM	(*)	61	118	6	14	30	26
NO_3^-	<0.27 μM		57	119	24	67	28	29
N/P ratio	<16		72	135	13	22	26	18
TChl*a*[a]	<0.06 mg m^{-3}	(*)	3	17	43	18	9	52
TChl*a*[b]	0.06–0.1 mg m^{-3}		64	20	27	18	16	45
TChl*a*[c]	0.1–0.3 mg m^{-3}		35	19	39	18	30	31
TChl*a*[d]	>0.3 mg m^{-3}		28	11	38	19	6	55

Thresholds for temperature and inorganic nutrients were around the median value in the 62 MALASPINA and INDEMARES surface samples in order to obtain an equal number of samples in each category. Chlorophyll *a* ranges were established according to the trophic water classification of Shushkina *et al*., 1997. Asterisk (*) indicates when abundances values were significantly different ($P<0.05$; Mann–Whitney test) inside and outside the corresponding range.
[a]Ultraoligotrophic.
[b]Oligotrophic.
[c]Mesotrophic.
[d]Eutrophic.

Therefore, we consider that the 1:1 UCYN-A1/host ratio is the most plausible assumption for estimating N host requirements and metabolite exchanges between partner cells and evaluating the contribution of this partnership to N_2 fixation. In addition, we suggest that the presence of two UCYN-A1 cells per host may derive from repartition of symbionts before host cell division. We made punctual captures of host cells likely displaying different stages of cell division (Supplementary Figure S5). It is known from field (Jacquet *et al*., 1998) and laboratory studies (Jacquet *et al*., 2001) that photosynthetic picoeukaryotes divide during a very short time window just before or during the dark period. We detected two cells per host mostly in INDEMARES samples, which were collected after sunset and thus the symbiotic population could be in active cell division. In the future, microscopic observations during diel cycles coupled with transcriptomic analyses would shed light on the division mechanisms within this symbiosis.

A widespread distribution of the symbiosis in the marine ecosystem

The distribution obtained based on CARD-FISH counts, together with the 18S rDNA metabarcoding from the circumglobal expedition *Tara*-Oceans, expands the geographic distribution of the symbiosis and presents contrasted ecological patterns of both types. The UCYN-A1 host appeared in few spots of high abundance and was undetected in ~56% of CARD-FISH surface samples. The distribution of this host based on V9 reads supported this patchy distribution. Although the metabarcoding method has a much lower detection limit than the CARD-FISH method, we could not detect the presence of UCYN-A1 host reads in a substantial number of stations (~62%). The UCYN-A2 host was detected only occasionally by CARD-FISH, likely because its abundance was below the detection threshold, consistent with reported cell abundances of *B. bigelowii* of up to 1 cells ml^{-1} in marine systems (Konno *et al*., 2007). This limitation to obtain a reliable signal of the UCYN-A2 host was offset with the metabarcoding approach. Thus the UCYN-A2 host showed an unexpected homogeneous distribution at low relative abundance in the open ocean, with targeted reads detected throughout *Tara*-Oceans samples.

Our CARD-FISH observations expanded the geographic coverage of UCYN-A1 in symbiosis to the South Atlantic gyre and the southern Indian Ocean. In these regions, no records of the prymnesiophyte phylotypes or UCYN-A were documented previously, except occasional detections of UCYN-A *nifH* sequences (no clade distinction) in the Benguela upwelling system, in the Arabian Sea and near Madagascar (Mazard *et al*., 2004; Moisander *et al*., 2010; Sohm *et al*., 2011a). Moreover, our metabarcoding analysis represented the first detection of both hosts in the Red Sea and widened the presence of the UCYN-A2 host in the South Pacific, the Arabian Sea and the Mediterranean Sea, where only few *nifH* clones of UCYN-A2 were reported (Man-Aharonovich *et al*., 2007). Previous reports showed that *B. bigelowii* usually occurred in low salinity, nutrient-rich coastal waters (Konno *et al*., 2007; Hagino *et al*., 2013), although it was also reported in the Sargasso Sea (Gaarder, 1954; Hulburt, 1962). Our study reinforces the presence of *B. bigelowii* in symbiosis with UCYN-A in open ocean stations, consistent with the finding of *nifH* copies of the UCYN-A2 phylotype in the open sea (Thompson *et al*., 2014).

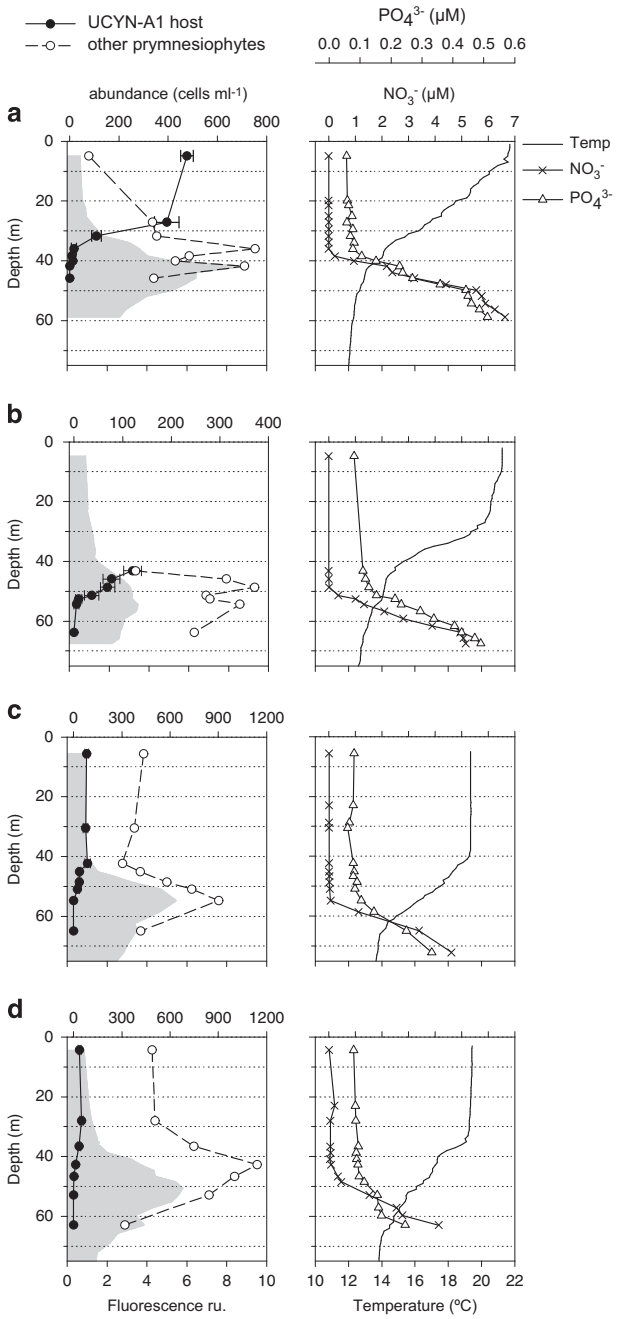

Figure 6 Depth profiles of hydrological variables (right) and distribution in depth of the prymnesiophyte–UCYN-A1 symbiosis (black dots) and the rest of the prymnesiophyte community (white dots) (left) for the INDEMARES stations in the NE Atlantic. Stations A and B correspond to the Avilés canyon region; stations C and D correspond to the Galician Bank region. The gray shaded area represents the fluorescence profile recorded at each station. Error bars represent s.e.

In the ocean, cyanobacterial diazotrophs generally show a consistent pattern in depth with higher abundances in the upper euphotic zone (Goebel *et al.*, 2010; Moisander *et al.*, 2010). Recurring summer blooms of these diazotrophs are reported in the North Pacific subtropical gyre (Dore *et al.*, 2008) usually related to shallow mixing conditions that ensure the solar energy needed for nitrogen fixation. A recent study showed that the UCYN-A symbiosis appeared largely restricted to the upper water column, where N/P ratios were <16 (Krupke *et al.*, 2014a). Our highly resolved vertical profiles show that (i) the prymnesiophyte–UCYN-A1 symbiosis occupies nutrient-depleted surface waters, and (ii) its abundance decreases in the shallow DCM. This pattern suggests a dependence on light intensity, and/or an out-competition of the symbiotic population by other non-diazotrophic species that benefit from the increased nutrient availability at the nutricline. This vertical pattern is comparable to that observed for UCYN-A1 *nifH* gene abundances in station ALOHA (Church *et al.*, 2005, 2009). In these vertical profiles, between 10^4-10^6 *nifH* copies per liter (roughly equivalent to 10–1000 cells ml^{-1}) were quantified in the well-lit, nutrient-depleted upper waters, and abundances decreased in the DCM to 10^2–10^3 *nifH* copies per liter (~1 cell ml^{-1}).

Environmental controls of cyanobacterial diazotrophs in the ocean

In our study, no environmental factor explained unambiguously the prymnesiophyte–UCYN-A1 distribution in surface waters. Presence or absence of the symbiosis occurred under similar environmental conditions (Supplementary Figure S4). Previous reports point to temperature as a driver of the distribution of cyanobacterial diazotrophs (Church *et al.*, 2008; Moisander *et al.*, 2010). Particularly for UCYN-A, *nifH* gene abundances have been reported to be higher in temperature ranges from 19 to 24 °C (Church *et al.*, 2008; Langlois *et al.*, 2008). Our study, with detections at a thermal range of 18–30 °C, revealed a weak negative relationship between symbiosis abundance and temperature, agreeing with previous reports. Limiting nutrients such as iron or phosphate might also control the distribution of cyanobacterial diazotrophs (Moore *et al.*, 2009; Sohm *et al.*, 2011b). Indeed, higher abundances of diazotrophs have been linked to oceanic areas where these nutrients are supplied from dust deposition of adjacent desert areas (Ridame and Guieu 2002; Tyrrell *et al.*, 2003; Capone *et al.*, 2005; Mahowald *et al.*, 2009). The patches of symbiosis observed in this study in the eastern North Atlantic, the western coast of Australia or even near Hawaii could be explained by deposition events, as high dissolved Fe concentrations have been reported in these areas (Brown *et al.*, 2005; Langlois *et al.*, 2012). Patchiness seems to be a common feature of diazotrophic populations (Church *et al.*, 2009; Goebel *et al.*, 2010), and UCYN-A is regarded as very dynamic over small spatio-temporal scales (Robidart *et al.*, 2014).

The regional dominance of different diazotrophic groups can be related to distinct temperature and nutrient requirements (Church *et al.*, 2008; Langlois *et al.*, 2008). For instance, in the tropical North Atlantic, *Trichodesmium* was dominant in the

warmer western side, whereas UCYN-A was more abundant in the cooler eastern side near Cape Verde Islands (Goebel *et al.*, 2010). During the MALASPINA expedition, a similar picture for the distribution of UCYN-A and *Trichodesmium* within this basin was observed, with these two diazotrophic groups dominating in different regions (see Fernández-Castro *et al.*, 2015 for a *Trichodesmium* distribution map). In addition, N_2-fixation rates measured during the MALASPINA expedition did not correlate with *Trichodesmium* abundances (Fernández-Castro *et al.*, 2015), but we noticed that regions of enhanced N_2-fixation rates as in the western South Atlantic or the eastern Indian ocean were coupled to the presence of prymnesiophyte–UCYN-A association. A recent latitudinal study along the eastern Australian coast also described a community shift from *Trichodesmium* in the north to unicellular diazotrophs in the south where the highest N_2-fixation rates were reported (Raes *et al.*, 2014).

Different ecological strategies between the two related lineages

Our results obtained by FISH counts and metabarcoding sequences in a large set of marine samples demonstrated that the two types of prymnesiophyte–UCYN-A symbiosis were widespread in the photic layer of the world ocean. We observed that UCYN-A2 host was homogeneously distributed at both surface and DCM but in low abundance, whereas UCYN-A1 host was only detected in some hotspots of very high abundance at surface, suggesting different ecological strategies. We hypothesize that UCYN-A1 host could follow the r strategy, with fast growth under favorable conditions, such as unpredictable events of dust deposition or the onset of thermal stratification, using surface light for the energy-demanding process of nitrogen fixation. On the other hand, the UCYN-A2 host could follow the k strategy (also known as stress-tolerant species by Reynolds, 1997), persisting at low abundances and being more competitive in stable and low-resource conditions. In this sense, the small UCYN-A1 host seems excluded in the DCM likely because other species are more efficient in waters with higher nutrients and dimmer light, while this depth limitation could be less severe in the UCYN-A2 host, which seems to be less affected by changes in the light regime (Thompson *et al.*, 2014). A better understanding of the role of UCYN-A diazotrophy along the vertical profile may certainly benefit from transcriptional profiles of these populations, including the mechanisms of the host to regulate UCYN-A activity. Overall, further studies on the biogeochemical role of the UCYN-A diazotrophy may need to include contrasted ecological differences among the different lineages.

Conflict of Interest

The authors declare no conflict of interest.

Acknowledgements

Financial support has been provided by the Spanish Ministry of Economy and Competitivity through project Consolider-Ingenio Malaspina 2010 (CSD2008-00077) to CMD, FLAME (CGL2010-16304) to RM, and PANGENOMICS (CGL2011-26848/BOS) to SGA. AMC was recipient of a Spanish FPI grant (BES-2009-027194). We thank all the technicians, researchers, crew and chief scientists of the different cruises for collaboration. We thank M Galindo and P de la Fuente for nutrient analysis, R Logares for sequence advice, R Simó and JM Gasol for useful comments on the manuscript and B Fernández-Castro and B Mouriño for sharing unpublished data.

References

Bombar D, Heller P, Sanchez-Baracaldo P, Carter BJ, Zehr JP. (2014). Comparative genomics reveals surprising divergence of two closely related strains of uncultivated UCYN-A cyanobacteria. *ISME J* **8**: 2530–2542.

Brown MT, Landing WM, Measures CI. (2005). Dissolved and particulate Fe in the western and central North Pacific: results from the 2002 IOC cruise. *Geochem Geophys Geosyst* **6**: Q10001.

Capone DG, Burns JA, Montoya JP, Subramaniam A, Mahaffey C, Gunderson T *et al.* (2005). Nitrogen fixation by *Trichodesmium* spp.: an important source of new nitrogen to the tropical and subtropical North Atlantic Ocean. *Glob Biogeochem Cycles* **19**: GB2024.

Carpenter EJ, Foster RA. (2002). Marine cyanobacterial symbiosis. In: Rai AN, Bergman B, Rasmussen U (eds). *Cyanobacteria in Symbiosis*. Kluwer Academic Publishers: Dordrecht, The Netherlands, pp 11–17.

Church MJ, Bjo KM, Karl DM, Saito MA, Zehr JP. (2008). Regional distributions of nitrogen-fixing bacteria in the Pacific Ocean. *Limnol Oceanogr* **53**: 63–77.

Church MJ, Jenkins BD, Karl DM, Zehr JP. (2005). Vertical distributions of nitrogen-fixing phylotypes at stn ALOHA in the oligotrophic North Pacific Ocean. *Aquat Microb Ecol* **38**: 3–14.

Church MJ, Mahaffey C, Letelier RM, Lukas R, Zehr JP, Karl DM. (2009). Physical forcing of nitrogen fixation and diazotroph community structure in the North Pacific subtropical gyre. *Glob Biogeochem Cycles* **23**: GB2020.

Cornejo-Castillo FM, Cabello AM, Salazar G, Sánchez-Baracaldo P, Lima-Mendez G, Hingamp P *et al.* Co-evolution and genome expression of closely related cyanobacterial symbionts originated during the late Cretaceous. (Submitted).

De Vargas C, Audic S, Henry N, Decelle J, Mahé F, Logares R *et al.* (2015). Eukaryotic plankton diversity in the sunlit ocean. *Science* **348**: 1261605.

Dore JE, Letelier RM, Church MJ, Lukas R, Karl DM. (2008). Summer phytoplankton blooms in the oligotrophic North Pacific Subtropical Gyre: historical perspective and recent observations. *Prog Oceanogr* **76**: 2–38.

Fernández-Castro B, Mouriño-Carballido B, Marañón E, Chouciño P, Gago J, Ramírez T *et al.* (2015). Important role of salt-finguers diffusivity for new nitrogen supply in oligotrophic ocean. *Nat Commun* (in press).

Foster RA, Carpenter EJ, Bergman B. (2006). Unicellular cyanobionts in open ocean dinoflagellates, radiolarians, and tintinnids: ultrastructural characterization and immuno-localization of phycoerythrin and nitrogenase. *J Phycol* **42**: 453–463.

Foster RA, Kuypers MMM, Vagner T, Paerl RW, Musat N, Zehr JP. (2011). Nitrogen fixation and transfer in open ocean diatom-cyanobacterial symbioses. *ISME J* **5**: 1484–1493.

Gaarder KR. (1954). Coccolithineae, Silicoflagellatae, Pterospermataceae and other forms from the "Michael Sars" North Atlantic Deep-Sea Expedition 1910. Report on the scientific results of the "Michael Sars" North Atlantic Deep-Sea Expedition. The Trustees of the Bergen museum: Bergen, Norway, pp 1–20.

Goebel NL, Turk KA, Achilles KM, Paerl R, Hewson I, Morrison AE *et al.* (2010). Abundance and distribution of major groups of diazotrophic cyanobacteria and their potential contribution to N_2 fixation in the tropical Atlantic Ocean. *Environ Microbiol* **12**: 3272–3289.

Grasshoff K, Ehrhardt M, Kremling K. (1999). *Methods of Seawater Analysis*, 3rd edn. Wiley-VCH: Weinheim, Germany.

Hagino K, Onuma R, Kawachi M, Horiguchi T. (2013). Discovery of an endosymbiotic nitrogen-fixing cyanobacterium UCYN-A in *Braarudosphaera bigelowii* (Prymnesiophyceae). *PLoS One* **8**: e81749.

Hagino K, Takano Y, Horiguchi T. (2009). Pseudo-cryptic speciation in *Braarudosphaera bigelowii* (Gran and Braarud) Deflandre. *Mar Micropaleontol* **72**: 210–221.

Hulburt EM. (1962). Phytoplankton in the southwestern Sargasso Sea and North Equatorial Current. *Limnol Oceanogr* **7**: 307–315.

Jacquet S, Lennon JF, Marie D, Vaulot D. (1998). Picoplankton population dynamics in coastal waters of the northwestern Mediterranean Sea. *Limnol Oceanogr* **43**: 1916–1931.

Jacquet S, Partensky F, Lennon JF, Vaulot D. (2001). Diel patterns of growth and division in marine picoplankton in culture. *J Phycol* **37**: 357–369.

Karsenti E, Acinas SG, Bork P, Bowler C, De Vargas C, Raes J *et al.* (2011). A holistic approach to marine ecosystems biology. *PLoS Biol* **9**: e1001177.

Konno S, Harada N, Jordan RW. (2007). Living *Braarudosphaera bigelowii* (Gran & Braarud) Deflandre in the Bering Sea. *J Nannoplankt Res* **29**: 78–87.

Krupke A, Lavik G, Halm H, Fuchs BM, Amann RI, Kuypers MMM. (2014a). Distribution of a consortium between unicellular algae and the N2 fixing cyanobacterium UCYN-A in the North Atlantic Ocean. *Environ Microbiol* **16**: 3153–3167.

Krupke A, Mohr W, LaRoche J, Fuchs BM, Amann RI, Kuypers MMM. (2014b). The effect of nutrients on carbon and nitrogen fixation by the UCYN-A-haptophyte symbiosis. *ISME J* **9**: 1635–1647.

Krupke A, Musat N, LaRoche J, Mohr W, Fuchs BM, Amann RI *et al.* (2013). In situ identification and N_2 and C fixation rates of uncultivated cyanobacteria populations. *Syst Appl Microbiol* **36**: 259–271.

Langlois RJ, Hümmer D, LaRoche J. (2008). Abundances and distributions of the dominant *nifH* phylotypes in the Northern Atlantic Ocean. *Appl Environ Microbiol* **74**: 1922–1931.

Langlois RJ, Mills MM, Ridame C, Croot P, LaRoche J. (2012). Diazotrophic bacteria respond to Saharan dust additions. *Mar Ecol Prog Ser* **470**: 1–14.

Latasa M. (2014). A simple method to increase sensitivity for RP-HPLC phytoplankton pigment analysis. *Limnol Oceanogr Methods* **12**: 46–53.

Mahowald NM, Engelstaedter S, Luo C, Sealy A, Artaxo P, Benitez-Nelson C *et al.* (2009). Atmospheric iron deposition: global distribution, variability, and human perturbations. *Ann Rev Mar Sci* **1**: 245–278.

Man-Aharonovich D, Kress N, Zeev EB, Berman-Frank I, Béjà O. (2007). Molecular ecology of *nifH* genes and transcripts in the eastern Mediterranean Sea. *Environ Microbiol* **9**: 2354–2363.

Mazard SL, Fuller NJ, Orcutt KM, Bridle O, Scanlan DJ. (2004). PCR analysis of the distribution of unicellular cyanobacterial diazotrophs in the Arabian Sea. *Appl Environ Microbiol* **70**: 7355–7364.

Moisander PH, Beinart RA, Hewson I, White AE, Johnson KS, Carlson CA *et al.* (2010). Unicellular cyanobacterial distributions broaden the oceanic N_2 fixation domain. *Science* **327**: 1512–1514.

Moore MC, Mills MM, Achterberg EP, Geider RJ, LaRoche J, Lucas MI *et al.* (2009). Large-scale distribution of Atlantic nitrogen fixation controlled by iron availability. *Nat Geosci* **2**: 867–871.

Moreno-Ostos E. (2012). Libro blanco de métodos y técnicas de trabajo oceanográfico. Expedición de circunnavegación Malaspina 2010: Cambio global y exploración de la biodiversidad del océano. CSIC: Madrid, Spain.

Nakayama T, Kamikawa R, Tanifuji G, Kashiyama Y, Ohkouchi N, Archibald JM *et al.* (2014). Complete genome of a nonphotosynthetic cyanobacterium in a diatom reveals recent adaptations to an intracellular lifestyle. *Proc Natl Acad Sci USA* **111**: 11407–11412.

Pernthaler A, Pernthaler J, Amann R. (2004). Sensitive multi-color fluorescence in situ hybridization for the identification of environmental microorganisms. *Mol Microb Ecol Man* **3**: 711–726.

Raes E, Waite A, McInnes A, Olsen H, Nguyen H, Hardman-Mountford N *et al.* (2014). Changes in latitude and dominant diazotrophic community alter N_2 fixation. *Mar Ecol Prog Ser* **516**: 85–102.

Rai AN, Bergman B, Rasmussen U. (2002). *Cyanobacteria in Symbiosis*. Kluwer Academic Publishers: Secaucus, NJ, USA.

Reynolds CS. (1997). *Vegetation Processes in the Pelagic: A Model for Ecosystem Theory*. International Ecology Institute: Oldendorf/Luhe, Germany.

Ridame C, Guieu C. (2002). Saharan input of phosphate to the oligotrophic water of the open western Mediterranean Sea. *Limnol Oceanogr* **47**: 856–869.

Robidart JC, Church MJ, Ryan JP, Ascani F, Wilson ST, Bombar D *et al.* (2014). Ecogenomic sensor reveals controls on N_2-fixing microorganisms in the North Pacific Ocean. *ISME J* **8**: 1175–1185.

Shi XL, Marie D, Jardillier L, Scanlan DJ, Vaulot D. (2009). Groups without cultured representatives dominate eukaryotic picophytoplankton in the oligotrophic South East Pacific Ocean. *PLoS One* **4**: e7657.

Shushkina EA, Vinogradov ME, Lebedeva LP, Anokhina LL. (1997). Productivity characteristics of epipelagic communities of the world's oceans. *Oceanology* **37**: 346–353.

Simon N, Campbell L, Ornolfsdottir E, Groben R, Guillou L, Lange M *et al.* (2000). Oligonucleotide probes for the identification of three algal groups by dot blot and fluorescent whole-cell hybridization. *J Eukaryot Microbiol* **47**: 76–84.

Sohm JA, Hilton JA, Noble AE, Zehr JP, Saito MA, Webb EA. (2011a). Nitrogen fixation in the South Atlantic Gyre and the Benguela Upwelling system. *Geophys Res Lett* **38**: L16608.

Sohm JA, Webb EA, Capone DG. (2011b). Emerging patterns of marine nitrogen fixation. *Nat Rev Microbiol* **9**: 499–508.

Thompson A, Carter BJ, Turk-Kubo K, Malfatti F, Azam F, Zehr JP. (2014). Genetic diversity of the unicellular nitrogen-fixing cyanobacteria UCYN-A and its prymnesiophyte host. *Environ Microbiol* **16**: 3238–3249.

Thompson AW, Foster RA, Krupke A, Carter BJ, Musat N, Vaulot D *et al.* (2012). Unicellular cyanobacterium symbiotic with a single-celled eukaryotic alga. *Science* **337**: 1546–1550.

Tripp HJ, Bench SR, Turk KA, Foster RA, Desany BA, Niazi F *et al.* (2010). Metabolic streamlining in an open-ocean nitrogen-fixing cyanobacterium. *Nature* **464**: 90–94.

Tyrrell T, Marañón E, Poulton AJ, Bowie AR, Harbour DS, Woodward EMS. (2003). Large-scale latitudinal distribution of Trichodesmium spp. in the Atlantic Ocean. *J Plankton Res* **25**: 405–416.

Yentsch CS, Menzel DW. (1963). A method for the determination of phytoplankton chlorophyll and phaeophytin by fluorescence. *Deep Sea Res Oceanogr Abstr* **10**: 221–231.

Zehr JP, Bench SR, Carter BJ, Hewson I, Niazi F, Shi T *et al.* (2008). Globally distributed uncultivated oceanic N_2-fixing cyanobacteria lack oxygenic photosystem II. *Science* **322**: 1110–1112.

Supplementary Information accompanies this paper on The ISME Journal website (http://www.nature.com/ismej)